TaKaRa Smart Cycler System and TaKaRa Ex Taq™ R-PCR ver. (TaKaRa, Shiga, Japan), where amplification of target DNA fragments were detected by the SYBR Green I method. The rat Multiple Tissue cDNA (MTC™) Panel I (Clontech, Palo Alto, CA) was used as the PCR template. Rat Abcc1 cDNA was specifically amplified under the following reaction conditions: 95°C for 30 s, 45 cycles of 95°C for 15 s, 55°C for 15 s, 72°C for 15 s, and 86°C for 7 s. For the reaction, the following rat *Abcc1* gene-specific PCR primers were used: sense primer sequence GGAATTTTCGACTAAGTGTCTATGG (q-rc1F), and anti-sense primer sequence TTGGAGAATCGGTTCACTAGG (q-rc1B).

Expression of Rat Abcc1 cDNA in HEK 293 Cells

The rat Abcc1 cDNA in the pcDNA3.1 vector (Invitrogen) was transfected into HEK 293 cells. Transfection was performed by using the LipofectAmine reagent (Invitrogen) according to the manufacturer's instruction. At 72 h after the start of transfection, cells were seeded into 10-cm culture dishes at several cell densities. G-418 disulfate (Nacalai Tesque, Kyoto, Japan) was added to the medium as a selection agent (final concentration 0.5 mg/ml). Three weeks later, single colonies were picked and subcultured. Positive colonies were selected by immunoblot analysis (see below). Growth of the transfected HEK 293 cells was maintained in Dulbecco's modified eagle's medium (Sigma-Aldrich Corp., St. Louis, MO) supplemented with 10% heat-inactivated fetal calf serum, penicillin (100 U/ml) and streptomycin (0.1 mg/ml) in a humidified chamber (37°C, 5% CO_2). The number of living cells was determined in a hemocytometer by Trypan Blue dye exclusion.

Immunoblot Analysis

The expression of rat Abcc1 in HEK 293 cells was examined by immunoblot analysis. Approximately 1×10^6 cells were treated with 0.1 ml of the cell lysis buffer containing 0.1% SDS and 1% NP-40. Protein concentrations were determined by using the BCA Protein Assay Kit (PIERCE, Rockford, IL). Samples (10 μg of proteins) were separated on 7.5% SDS-PAGE gels and electro-blotted onto PVDF membranes (Amersham Biosciences, Buckinghamshire, UK). Blots were probed with rat Abcc1-specific antibody, MRPr1 (1:300 dilution; IQProduct, Houston, TX) and subsequently with peroxidase-conjugated AffiniPure mouse anti-rat immunoglobulin G (IgG) (dilution 1:5000; Jackson ImmunoResearch Laboratories, Inc. West Grove, PA).

Drug-Resistance Profile

HEK 293 cells were seeded in 96-well plates at a density of 2000 cells/well in 0.1 ml of volume. After 24 h, 5 μl of drugs was added at various concentrations. Drugs were diluted in phosphate-buffered saline (PBS). An equal volume (5 μl) of PBS was added to the control wells. The MTT (3-(4,5-dimethylthiazol-2-yl)-2,5-diphenyltetrazolium bromide) method was used to determine chemosensitivity to chemotherapeutic drugs. After 72 h, 10 μl of 5 mg/ml MTT (Sigma-Aldrich, St. Louis, MO) was added and incubated at 37°C for 4 h. The incubation medium was discarded and 0.1 ml of dimethyl sulfoxide was then added to dissolve both cells and formazan, a metabolite of MTT. Thereafter, the absorbance was photometrically measured at a test wavelength of 570 nm and a reference wavelength of 630 nm with a 96-well plate reader.

Drugs

Doxorubicin, daunorubicin, vincristine, vinblastine, colchicine, methotrexate, mitomycin C, and actinomycin D were purchased from Wako Pure Chemical Industries (Osaka, Japan). Etoposide and mitoxantrone were from Sigma-Aldrich (St. Louis, MO). Epirubicin was from ICN Biomedicals Inc. (Aurora, OH).

Computer Analysis

BLAST search in the NCBI rat genome database (http://www.ncbi.nlm.nih.gov/genome/seq/RnBlast.html) was used to obtain partial genomic DNA sequences. GENETYX-WIN Version 5.1 was used for homology analysis and multiple alignment analysis. BLAT search in the UCSC Genome Bioinformatics (http://genome.cse.ucsc.edu/) was used to determine the genome localization. The

SOSUI program (http://sosui.proteome.bio.tuat.ac.jp/sosuiframe0.html) was used to predict transmembrane domains.

RESULTS

Molecular Cloning of Rat Abcc1 cDNA

Figure 1 depicts the strategy of cloning rat Abcc1 cDNA. By referring to the rat genome sequence data and the mouse Abcc1 cDNA sequence (GenBank accession number: AF020908), we first designed PCR primers to obtain three partial fragments that cover the open reading frame (ORF) of rat Abcc1. The sequences of the three PCR products were analyzed and confirmed by using the rat genome database. The BLAT search on the rat genome has revealed that the rat *Abcc1* gene is located on the rat chromosome 13.

The rat Abcc1 cDNA (AF487549) thus cloned covered 4981-bp and the ORF (4599 bp) encodes 1532 amino acid residues. The cDNA sequence of rat Abcc1 was homologous with human ABCC1 and mouse Abcc1. In terms of amino acid sequence, the identity of rat Abcc1 with human ABCC1 and mouse Abcc1 was 87.3 and 95.1%, respectively. Figure 2 demonstrates the multiple alignments with the amino acid sequences of rat Abcc1, human ABCC1, and mouse Abcc1. Transmembrane domain prediction with the SOSUI program indicated that the full-length rat Abcc1 protein has a total of 17 transmembrane domains, being consistent with those of the human ABCC1 and mouse Abcc1 (Figure 2).

Splicing Variants

During the process of cloning Abcc1 cDNA, we have found two splicing variants (GenBank accession numbers: variants A, AY174892 and variant B, AY174893). Variants A and B lack 27-bp and 127-bp partial sequences, respectively, as compared with the full-length cDNA, and they encode 1523 and 698 amino acid residues, respectively. The predicted protein structures are schematically described in Figure 3A. Variant A lacks nine amino acid residues (912-QRHLSNSSS-920) located in the intracellular loop close to the first NBD. On the other hand, variant B involves a frame-shift in its cDNA sequence such that a translation stop codon becomes located between the walker A and signature C motifs. Therefore, variant B encodes a short peptide (698 amino acid residues), as indicated in Figure 3A.

To measure the expression levels of variants A and B as well as of the full-length Abcc1, we have carried out PCR with specific primers as shown in Figure 1B and C. The transcript of variant A was observed in all tissues tested, and its expression levels were comparable to those of the full-length Abcc1 (Figure 3B). On the other hand, the transcript of variant B was detected in heart, brain, spleen, and skeletal muscle, and its expression levels were much lower than those of the full-length Abcc1 (Figure 3C).

Quantitative PCR Analysis

Tissue-specific expression of the rat *Abcc1* gene was analyzed by using quantitative PCR (Figure 4). The rat Abcc1 transcript was specifically amplified with the PCR primers, i.e., q-rc1F and q-rc1B (Figure 1A). Prominent expression of rat Abcc1 was observed in the spleen with a copy number of 11,076, which is 4.3-fold higher than that observed in skeletal muscle, the tissue showing the second highest number (2586 copies). The copy numbers of rat Abcc1 in heart, lung, brain, kidney, and liver were 1690, 946, 481, 260, and 256, respectively. The expression in testis was the lowest (142 copies) among the tissues tested.

Expression of Rat Abcc1 in HEK 293 Cells

The rat Abcc1 protein was stably expressed in HEK 293 cells by transfection with the recombinant pcDNA3.1 vector encoding the full-length cDNA (see *Materials and Methods*). The expressed protein having a molecular mass of 190 kDa was detected with the MRPr1 antibody specific to rat Abcc1 (Figure 5A). Mock-transfected cells, as the negative control, did not show any immunologic reaction.

Drug-Resistance Profile of Rat Abcc1-Expressing HEK 293 Cells

Figure 5B and Table 1 show the drug-resistance profiles of rat Abcc1-expressing HEK 293 cells assessed by the MTT method.

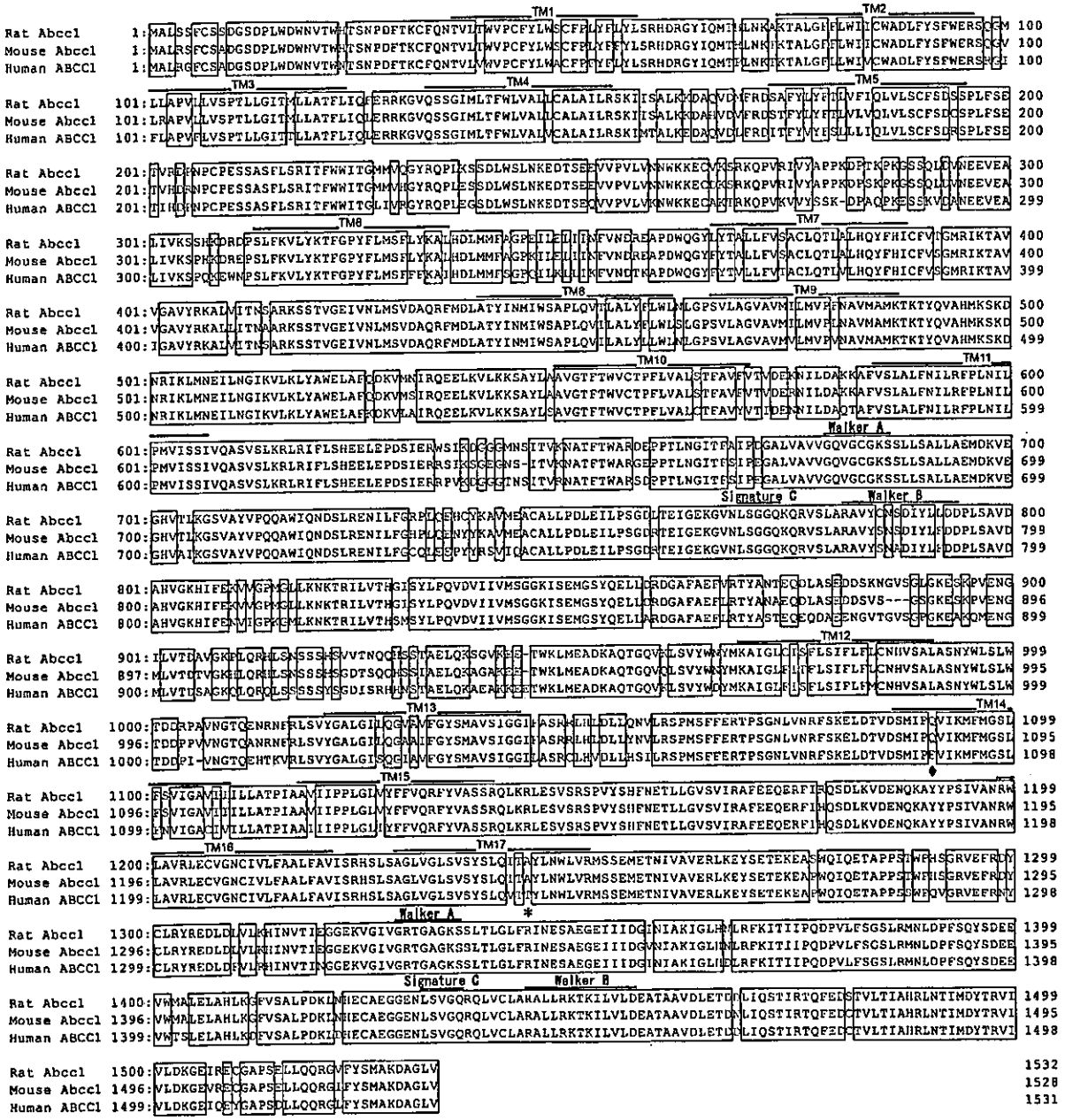

Figure 2. Multiple alignment analysis of rat Abcc1 protein with mouse Abcc1 protein and human ABCC1 protein. The multiple alignment among rat Abcc1, mouse Abcc1 (AF022908) and human ABCC1 (NM004996) was analyzed by using the GENETYX-WIN 5.1 software. Amino acid residues that are identical among these ABC transporters are indicated by boxes. Transmembrane domains were predicted by using the SOSUI program (http://sosui.proteome.bio.tuat.ac.jp/sosuiframe0.html), and they are indicated by over-lines as TM1–TM17 in the figure. ATP-binding domains are indicated by Walker A, Walker B, and Signature C. Amino acid residues critical for the activity are shown by diamond and asterisk symbols.

Overexpression of rat Abcc1 resulted in a remarkable increase (10.4-fold) in the cellular resistance to etoposide (VP-16) as compared with mock-transfected cells. A small, but statistically significant ($P < 0.01$), resistance to methotrexate was observed in the rat Abcc1-transfected HEK 293 cells (Table 1). While slight increases were observed in the resistance of Abcc1-expressing cells to doxorubicin, daunorubicin, mitoxantrone, and colchicine, these resistance factors were not statistically significant under the condition of $P < 0.01$ (Table 1). Likewise, there was no significant increase in cellular resistance to

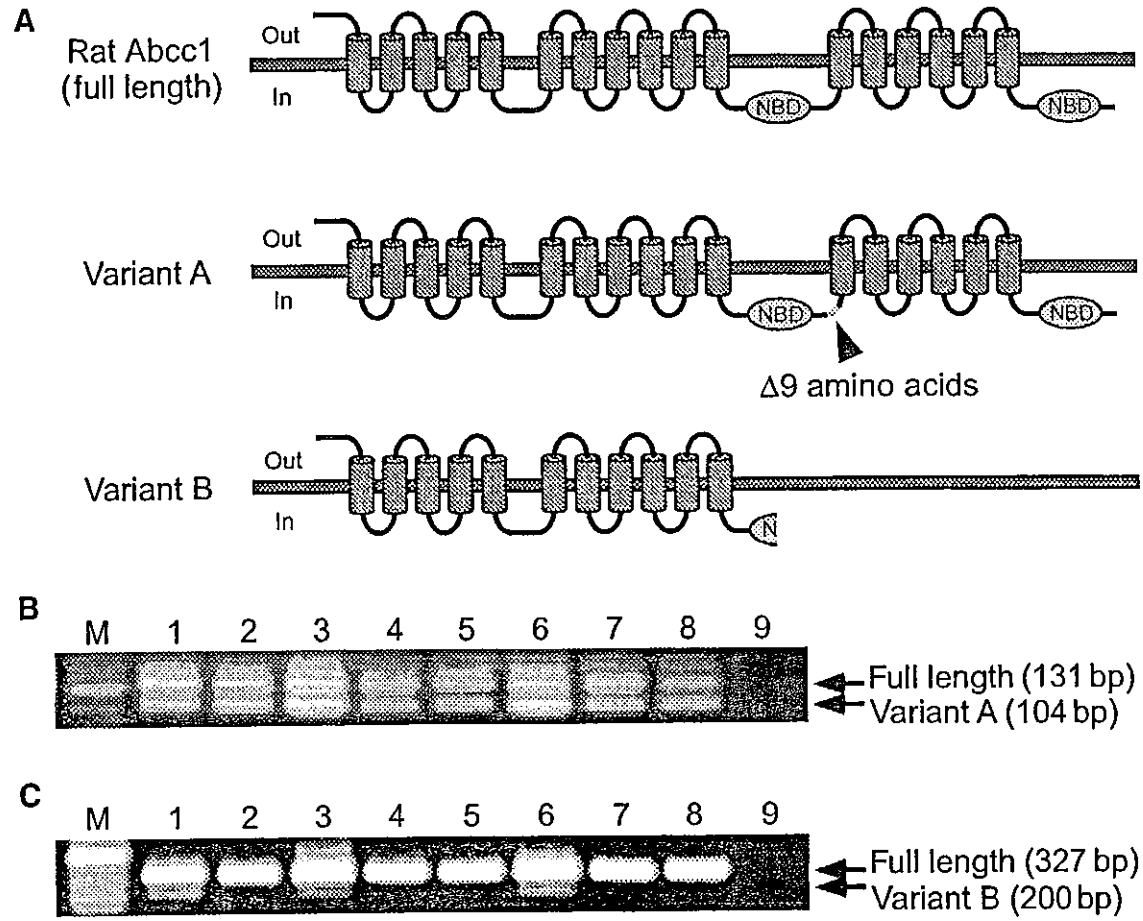

Figure 3. Alternative splicing in the rat Abcc1 gene. **(A)** Schematic illustration of putative protein structures of the full-length rat Abcc1 and splicing variants. The triangle indicates the deletion of nine amino acid residues in variant A. NBD, nucleotide-binding domain. **(B)** Expression levels of the full-length rat Abcc1 and variant A detected by PCR. Primers, −27-rc1F and −27-rc1B, were used for the polymerase chain reaction (PCR) (38 cycles) detection. The size of PCR products: 131 bp (full-length Abcc1), 104 bp (variant A). **(C)** Expression levels of the full-length rat Abcc1 and variant B detected by PCR. Primers, −127-rc1F and −127-rc1B, were used for the PCR (42 cycles) detection. The size of PCR products: 327 bp (full-length Abcc1), 200 bp (variant B). M, DNA marker; 1, heart; 2, brain; 3, spleen; 4, lung; 5, liver; 6, skeletal muscle; 7, kidney; 8, testis; 9, negative control.

vincristine, vinblastine, actinomycin D, mitomycin C, and epirubicin.

DISCUSSION

Cloning of Rat Abcc1 cDNA

The present study addresses the cloning and characterization of the cDNAs of rat Abcc1 and its splicing variants. In earlier studies, we first reported the existence of an ATP-dependent transport system in rat heart for the elimination of GSSG, glutathione conjugates, and leukotriene C_4 from cardiac cells (15,16). The transport system was named "GS-X pump", although its molecular nature was not identified at that time [4]. Successive studies of Müller et al. (17) and Jedlitschky et al. (18) have provided evidence that the GS-X pump is encoded by the ABCC1 (MRP1) gene originally cloned by Cole et al. [3].

To date, one partial sequence of the rat Abcc1 cDNA was reported by Keppler (GenBank accession number: AJ277881). The sequence was only 2969-bp long and did not include the translation start codon. In this context, we tried to obtain the full-length sequence of rat Abcc1 cDNA. Molecular cloning of the full-length cDNA (4981 bp) of rat Abcc1 was successfully achieved in the present study. We submitted its sequence to the GenBank (AF487549) on February 26, 2002. After our submission of the sequence, Yang

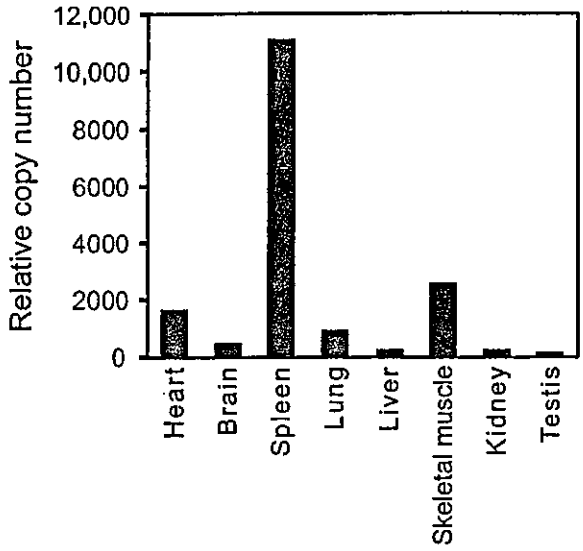

Figure 4. Expression levels of the rat *Abcc1* gene in different tissues, i.e., heart, brain, spleen, lung, liver, skeletal muscle, kidney and testis, as measured by quantitative polymerase chain reaction. Primers, q-rc1F and q-rc1B (Fig. 1A), were used for the quantitative PCR (see *Materials and methods*).

et al. (19) also reported the sequence of rat Abcc1 cDNA (AY170916). However, their sequence was 4599-bp long without 5′- and 3′-untranslated regions (UTR), and it contained a total of six mismatches as compared with our sequence. Furthermore, importantly, the sequence (AY170916) of Yang et al. contains partial sequences of mouse Abcc1 cDNA, since they have designed the 5′-end PCR primer (5′-ATGGCGCTGCG-CAGCTTCTGC-3′) based on the mouse Abcc1 cDNA sequence (AF020908). The sequence should be 5′-ATGGCGCTGAG-CAGCTTCTGC-3′ based on the rat genome sequence as well as on our cDNA sequence (AF487549).

The rat *Abcc1* gene is located on chromosome 13. While the current database of the rat genome sequence is not complete, the tentative structure of the rat *Abcc1* gene could be predicted by a BLAT search with our cDNA sequences. In the present study, two splicing variants were also discovered (Figure 1B and C). It is suggested that both the full-length rat Abcc1 and the variant A have at least 30 exons, whereas variant B may have at least 28 exons. Both the full-length rat Abcc1 and the variant A have two NBDs, whereas variant B does not (Figure 2A).

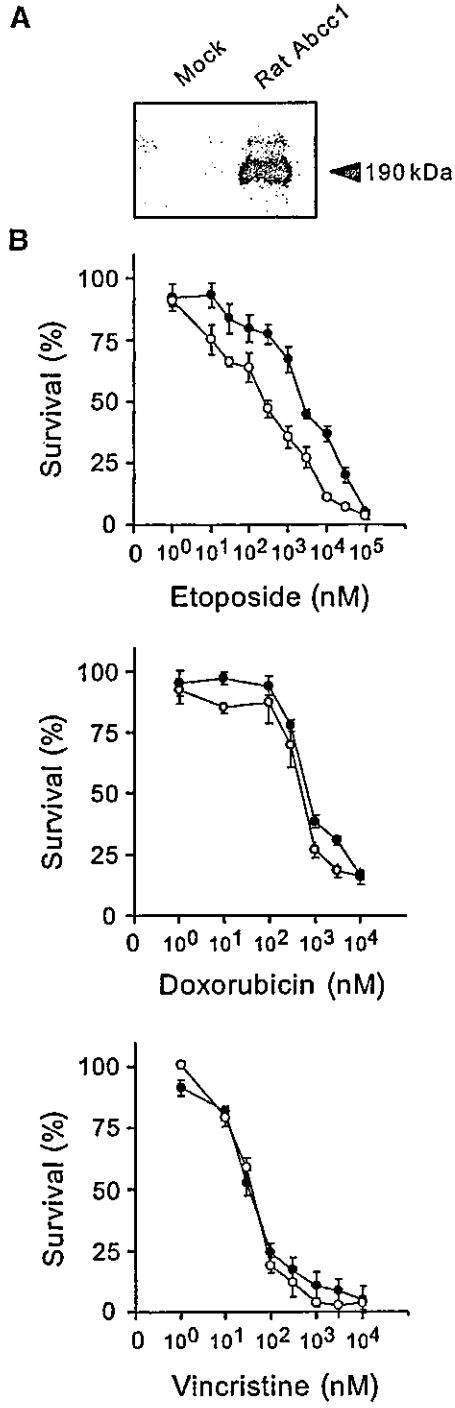

Figure 5. Immunoblot analysis and drug-resistance profiles of rat Abcc1-transfected HEK 293 cells. (A) Proteins (10 μg) were separated on a 7.5% SDS-PAGE gel, and rat Abcc1 protein was immunologically detected by using the MRPr1 antibody, as described in *Materials and methods*. (B) The cellular resistance of rat Abcc1-expressing HEK 293 cells (closed circles) and mock-transfected cells (open circles). Drugs tested were etoposide, doxorubicin, and vincristine as indicated in the figure. Cell viability was analyzed by the 3-(4,5-dimethylthiazol-2-yl)-2,5-diphenyltetrazolium bromide (MTT) method (see *Materials and methods*). Data are expressed as mean values±SD of triplicate measurements.

Table 1: Drug-resistance profile of rat Abcc1-overexpressing HEK 293 cells

Drugs	IC^a_{50} [nM]		Resistance Factor[b]
	Rat Abcc1	Mock	
Etoposide	8944±1334	871±78	10.4[c]
Doxorubicin	234.6±58.4	108±53	2.39
Daunorubicin	215.2±89.0	82.0±2.9	2.60
Epirubicin	69.4±12.8	58.7±26.0	1.35
Vincristine	73.2±31.7	49.5±12.9	1.52
Vinblastine	79.9±16.1	82.4±14.1	1.01
Methotrexate	207.5±49.7	83.4±12.3	2.45[c]
Actinomycin D	71.9±20.6	62.6±5.1	1.17
Mitomycin C	66.5±25.0	70.5±32.8	1.19
Mitoxantrone	95.6±59.1	55.1±29.2	1.78
Colchicine	62.3±10.9	22.7±3.9	2.74

[a]Drug concentrations that inhibit cell growth by 50%.

$$\frac{IC_{50} \text{ value (rat Abcc1-transfected HEK 293 cells)}}{IC_{50} \text{ value (mock-transfected cells)}}$$

[b]The drug-resistance profiles of rat Abcc1-transfected HEK 293 cells and mock-transfected cells were analyzed by the (3-(4,5-dimethylthiazol-2-yl)-2,5-diphenyltetrazolium bromide (MTT) method, as described in *Materials and methods*. Cells were incubated with drugs at 37°C for 72h. Data are expressed as mean values±SD in multiple experiments ($n \geq 3$). The statistical significance was examined by Student *t* test ([c]$P < 0.01$).

Expression Profiles of Rat Abcc1 and its Splicing Variants

In the present study, tissue distribution of rat Abcc1 expression was examined by quantitative PCR with the rat Multiple Tissue cDNA panel. Our results are substantially consistent with the ubiquitous expression profiles of human ABCC1 [20] and mouse Abcc1 [21]. In the present study, however, the highest expression of rat Abcc1 was observed in the spleen (Figure 4). Skeletal muscle and heart were the second and third highest organs, supporting our previous findings of ATP-dependent transport of glutathione conjugates from the rat heart (15,16). The characteristically high expression level of rat Abcc1 in the spleen implicates an association of rat Abcc1 with certain physiological functions. It has recently been reported that mouse Abcc1 regulates CCL19-dependent mobilization of dendritic cells to lymph nodes [22].

In addition to the full-length rat Abcc1, we have discovered two splicing variants. The tissue distribution of variant A (Figure 3B) showed its ubiquitous expression, and its expression levels in the organs tested (heart, brain, spleen, lung, liver, skeletal muscle, kidney, and testis) were comparable to those of full-length rat Abcc1. Colony-directed PCR with the same primers, i.e., −27bp-rc1F and −27bp-rc1B, supported our findings (data not shown). Deletion of nine amino acid residues may affect the substrate specificity and/or the activity of Abcc1. The function of variant A remains to be elucidated in future studies.

Drug-Resitance Profile of Rat Abcc1 and Species Difference

The present study demonstrates that overexpression of rat Abcc1 confers HEK 293 cells resistance to etoposide (Figure 5, Table 1). It has previously been documented that human ABCC1 elicits resistance to a wide variety of chemotherapeutic drugs, such as doxorubicin, daunorubicin, vincristine, vinblastine, and etoposide [23]. Interestingly, however, overexpression of rat Abcc1 was not associated with cellular resistance to doxorubicin, vincristine, or vinblastine, as demonstrated in Figure 5 and Table 1. Although the rat Abcc1 protein exhibits a high homology (87.3%) with human ABCC1 in terms of the amino acid identity, there may be species differences in the function of rat Abcc1 and human ABCC1.

Until now, several ABCC1 orthologs have been cloned from bovine [24], canine [25],

Table 2: Drug-resistance profiles of ABCC1 orthologs cloned from different species and their critical amino acid residues

Species	Host cells	Amino acid	Drug		
			Etoposide	Doxorubicin	Vincristine
Human[a]	HEK 293	Glu (E) 1089 Thr (T) 1242	Resistant	Resistant	Resistant
Bovine[b]	KB3-1	Gln (Q) 1088 Thr (T) 1241	Resistant	Nil	Resistant
Canine[c]	HeLa	Gln (Q) 1090 Thr (T) 1244	Resistant	Nil	Nil
Mouse[a]	HEK 293	Gln (Q) 1086 Ala (A) 1239	Resistant	Nil	Resistant
Rat[d]	HEK 293	Gln (Q) 1090 Ala (A) 1244	Resistant	Nil	Nil

[a]Ref. 23.
[b]Ref. 24.
[c]Ref. 25.
[d]This study.

mouse [21], and rat (this study). It is of particular importance to note that there are some inconsistencies in the drug-resistance profiles among those ABCC1 orthologs. As demonstrated in Table 2, it is only human ABCC1 that can exhibit resistance to doxorubicin, while all orthologs represented in the table confer cellular resistance to etoposide.

The difference in the drug resistance to anthracyclines has previously been reported for human ABCC1 and mouse Abcc1 [23]. Mutational analyses of mouse Abcc1 and human ABCC1 revealed that two amino acid residues are critical for their activity (26,27). One is glutamate (Glu) at position 1089 in human ABCC1, corresponding to glutamine (Gln)-1086 in mouse Abcc1. The other is threonine (Thr)-1242 in human ABCC1, corresponding to alanine (Ala)-1239 in mouse Abcc1. By site-directed mutagenesis, Zhang et al. (26) suggested that the difference between Glu-1089 in human ABCC1 and Gln-1086 in mouse Abcc1 are closely related to drug resistance to anthracyclines. Indeed, ABCC1 orthologs with Gln at position 1088 (bovine) or 1090 (canine and rat) do not confer doxorubicin resistance (Table 2).

It has also been shown by mutational analysis of human ABCC1 and mouse Abcc1 that the combination of Gln-1086 and Ala-1239 in mouse Abcc1 and Glu-1089 and Thr-1242 in human ABCC1 is required to confer resistance to vincristine [27]. As demonstrated in Table 2, rat Abcc1 has Gln-1090 and Ala-1244. However, it does not exhibit resistance to vincristine. Therefore, it is likely that there are other critical amino acid residues that determine vincristine resistance.

CONCLUSION

Molecular cloning of rat Abcc1 was achieved in this study. In addition, two splicing variants were identified. The amino acid sequence of rat Abcc1 exhibited high homology with human ABCC1 and mouse Abcc1. The highest expression of the rat *Abcc1* gene was observed in the spleen. Overexpression of rat Abcc1 conferred resistance to etoposide, as does human ABCC1; however, the drug-resistance profile of rat Abcc1 differs from that of human ABCC1. Rat Abcc1 did not confer significant cellular resistance to anthracyclins or *Vinca* alkaloids. Glu-1089 in human ABCC1 corresponds to Gln-1086 in rat Abcc1. This amino acid alteration, at least, may explain the difference in the drug-resistance profile to doxorubicin between human ABCC1 and rat Abcc1. In this context, it is important to consider the effects of such amino acid residues in determining the activity of ABCC1 orthologs in different species. Accordingly, experiments should be carefully designed and executed for the validation of the pharmacological and toxicological properties of drug candidates by using model animals, because of species differences in the actions of drug transporters.

ACKNOWLEDGEMENTS

The present study was supported by research grants of "Toxicoproteomics: Expression of ABC transporter genes and drug-drug interactions" (H14-Toxico-002) from the Japanese Ministry of Health and Welfare, the Grant-in-Aid for Creative Scientific Research (No. 13NP0401), and the Japan Society for the Promotion of Science (No. 14370754).

REFERENCE

1. Borst P, Evers R, Kool M, Wijinholds J. The multidrug resistance protein family. *Biochim Biophys Acta* 1461: 347–357, 1999.
2. Ishikawa T. Multidrug resistance: genomics of ABC transporters. In: Cooper DN, ed. *Encyclopedia of Human Genome. London: Nature Publishing Group,* 4: 154–160, 2003.
3. Cole SP, Bhardwaj G, Gerlach JH, et al. Overexpression of a transporter gene in a multidrug-resistant human lung cancer cell line. *Science* 258: 1650–1654, 1992.
4. Ishikawa T. The ATP-dependent glutathione S-conjugate export pump. *Trends Biochem Sci* 17: 463–468, 1992.
5. Leslie EM, Deeley RG, Cole SP. Toxicological relevance of the multidrug resistance protein 1, MRP1 (ABCC1) and related transporters. *Toxicology* 167: 3–23, 2001.
6. Kool M, van der Linden M, de Haas M, et al. MRP3, an organic anion transporter able to transport anti-cancer drugs. *Proc Natl Acad Sci USA* 96: 6914–6919, 1999.
7. Cui Y, Konig J, Buchholz JK, Spring H, Leier I, Keppler D. Drug resistance and ATP-dependent conjugate transport mediated by the apical multidrug resistance protein, MRP2, permanently expressed in human and canine cells. *Mol Pharmacol* 55: 929–937, 1999.
8. Zeng H, Bain LJ, Belinsky MG, Kruh GD. Expression of multidrug resistance protein-3 (multispecific organic anion transporter-D) in human embryonic kidney 293 cells confers resistance to anticancer agents. *Cancer Res* 59: 5964–5967, 1999.
9. Kusuhara H, Sugiyama Y. Role of transporters in the tissue-selective distribution and elimination of drugs: transporters in the liver, small intestine, brain and kidney. *J Control Release* 78: 43–54, 2002.
10. Yabuuchi H, Shimizu H, Takayanagi S, Ishikawa T. Multiple splicing variants of two new human ATP-binding cassette transporters, ABCC11 and ABCC12. *Biochem Biophys Res Commun* 288: 933–939, 2001.
11. Tammur J, Prades C, Arnould I, et al. Two new genes from the human ATP-binding cassette transporter superfamily, ABCC11 and ABCC12, tandemly duplicated on chromosome 16q12. *Gene* 273: 89–96, 2001.
12. Bera TK, Lee S, Salvatore G, Lee B, Pastan I. MRP8, a new member of ABC transporter superfamily, identified by EST database mining and gene prediction program, is highly expressed in breast cancer. *Mol Med* 7: 509–516, 2001.
13. Bera TK, Iavarone C, Kumar V, Lee S, Lee B, Pastan I. MRP9, an unusual truncated member of the ABC transporter superfamily, is highly expressed in breast cancer. *Proc Natl Acad Sci USA* 99: 6997–7002, 2002.
14. Yabuuchi H, Takayanagi S, Yoshinaga K, Taniguchi N, Aburatani H, Ishikawa T. ABCC13, an unusual truncated ABC transporter, is highly expressed in fetal human liver. *Biochem Biophys Res Commun* 299: 410–417, 2002.
15. Ishikawa T, Sies H. Cardiac transport of glutathione disulfide and S-conjugate. Studies with isolated perfused rat heart during hydroperoxide metabolism. *J Biol Chem* 259: 3838–3843, 1984.
16. Ishikawa T. ATP/$Mg2^{+}$-dependent cardiac transport system for glutathione S-conjugates. A study using rat heart sarcolemma vesicles. *J Biol Chem* 264: 17343–17348, 1989.
17. Müller M, Meijer C, Zaman GJ, Borst P, Scheper RJ, Mulder NH, de Vries EG, Jansen PL. Overexpression of the gene encoding the multidrug resistance-associated protein results in increased ATP-dependent glutathione S-conjugate transport. *Proc Natl Acad Sci USA* 91: 13033–13037, 1994.
18. Jedlitschky G, Leier I, Buchholz U, Barnouin K, Kurz G, Keppler D. Transport of glutathione, glucuronate, and sulfate conjugates by the MRP gene-encoded conjugate export pump. *Cancer Res* 56: 988–994, 1996.
19. Yang Z, Li CS, Shen DD, Ho RJ. Cloning and characterization of the rat multidrug resistance-associated protein 1. *AAPS PharmSc* 4: E15, 2002.
20. Kool M, de Haas M, Scheffer GL, Scheper RJ, van Eijk MJ, Juijn JA, Baas F, Borst P. Analysis of expression of cMOAT (MRP2), MRP3, MRP4, and MRP5, homologues of the multidrug resistance-associated protein gene (MRP1), in human cancer cell lines. *Cancer Res* 57: 3537–3547, 1997.
21. Stride BD, Valdimarsson G, Gerlach JH, Wilson GM, Cole SP, Deeley RG. Structure and expression of the messenger RNA encoding the murine multidrug resistance protein, an ATP-binding cassette transporter. *Mol Pharmacol* 49: 962–971, 1996.
22. Robbiani DF, Finch RA, Jager D, Muller WA, Sartorelli AC, Randolph GJ. The leukotriene C4 transporter MRP1 regulates CCL19 (MIP-3beta, ELC)-dependent mobilization of dendritic cells to lymph nodes. *Cell* 103: 757–768, 2000.
23. Stride BD, Grant CE, Loe DW, Hipfner DR, Cole SP, Deeley RG. Pharmacological characterization of the murine and human orthologs of multidrug-resistance protein in transfected human embryonic kidney cells. *Mol Pharmacol* 52: 344–353, 1997.
24. Taguchi Y, Saeki K, Komano T. Functional analysis of MRP1 cloned from bovine. *FEBS Lett* 521: 211–213, 2002.
25. Ma L, Pratt SE, Cao J, Dantzig AH, Moore RE, Slapak CA. Identification and characterization of the canine multidrug resistance-associated protein. *Mol Cancer Ther* 1: 1335–1342, 2002.
26. Zhang DW, Cole SP, Deeley RG. Identification of an amino acid residue in multidrug resistance protein 1 critical for conferring resistance to anthracyclines. *J Biol Chem* 276: 13231–13239, 2001.
27. Zhang DW, Cole SP, Deeley RG. Identification of a non-conserved amino acid residue in multidrug resistance protein 1 important for determining substrate specificity: evidence for functional interaction between transmembrane helices 14 and 17. *J Biol Chem* 276: 34966–34974, 2001.

Available online at www.sciencedirect.com
SCIENCE DIRECT®
Journal of Chromatography B, 795 (2003) 25–34
JOURNAL OF CHROMATOGRAPHY B
www.elsevier.com/locate/chromb

Simple non-ion-paired high-performance liquid chromatographic method for simultaneous quantitation of carboxylate and lactone forms of 14 new camptothecin derivatives

Kazumi Sano[a,*], Megumi Yoshikawa[a], Shinya Hayasaka[a], Kurita Satake[a], Yoji Ikegami[a], Hisahiro Yoshida[a], Toshihisa Ishikawa[b], Seigo Sawada[c], Shinzo Tanabe[d]

[a]*Department of Drug Metabolism and Disposition, Meiji Pharmaceutical University, 2-522-1 Noshio, Kiyose-si, Tokyo 204-8588, Japan*
[b]*Department of Biomolecular Engineering, Graduate School of Bioscience and Biotechnology, Tokyo Institute of Technology, Yokohama, Japan*
[c]*Yakult Central Institute for Microbiological Research, Tokyo, Japan*
[d]*Department of Analytical Biochemistry, Meiji Pharmaceutical University, Kiyose, Tokyo, Japan*

Received 13 March 2003; received in revised form 22 May 2003; accepted 10 June 2003

Abstract

SN-38 (7-ethyl-10-hydroxycamptothecin) is an active metabolite derived from the semi-synthetic compound camptothecin (CPT) named Irinotecan (CPT-11). The antitumor activity of SN-38 is 1000-fold more potent than the parent CPT-11. Fourteen new derivatives of camptothecin have recently been developed by Yakult Honsha (Tokyo, Japan). Here we describe a simple and cost-effective high-performance liquid chromatography (HPLC) method without an ion-pairing agent, which allows the simultaneous determination of both lactone and carboxylate forms of SN-38 and other camptothecin derivatives. A weak linear relationship between the HPLC retention factors (ln k') and the cellular concentrations of these compounds was observed. These results suggest that low-polarity compounds easily accumulate in cancer cells and may circumvent drug resistance. The HPLC analysis herein described is expected to greatly assist in derivative synthesis and chemical modification of camptothecin-based antitumor drugs.

Keywords: Derivatization, LC; Camptothecin; SN-38; CPT-11

1. Introduction

Irinotecan hydrochloride (CPT-11) is a water-soluble derivative of camptothecin (CPT) [1]. CPT is a potent antitumor alkaloid extracted from the Chinese tree *Camptotheca acuminata* [2]. The antitumor activity of CPT is due to irreversible inhibition of DNA topoisomerase I (Topo I) [3–6]. However, clinical use of CPT was discontinued due to its high toxicity, and the water-soluble analog CPT-11 was developed. CPT-11 is metabolized in vivo by carboxyesterase to produce 7-ethyl-10-hydroxy-camptothecin (SN-38), an active metabolite. This metabolite is 1000-fold more potent than the parent compound in vitro [7,8].

SN-38 has an α-hydroxy-δ-lactone ring that under-

*Corresponding author. Tel.: +81-424-958-470; fax: +81-424-958-469.
E-mail address: ksano@my-pharm.ac.jp (K. Sano).

1570-0232/03/$ – see front matter
doi:10.1016/S1570-0232(03)00485-9

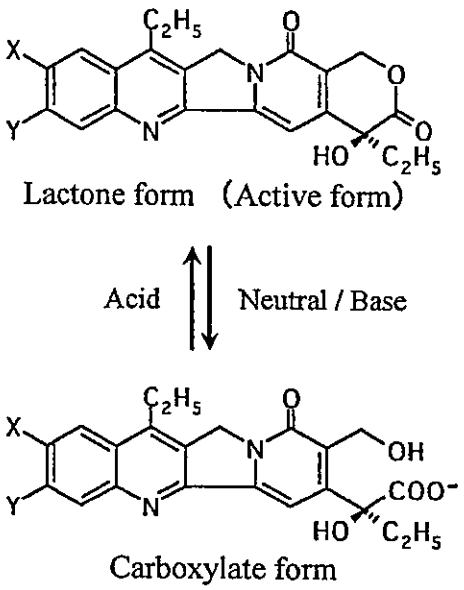

Fig. 1. Molecular structure of the lactone and carboxylate forms of SN-38.

goes reversible hydrolysis (Fig. 1) at a rate dependent on pH, ionic strength and protein concentration [9,10]. Human serum albumin (HSA) preferentially binds the carboxylate form over the lactone form with a 150-fold higher affinity. These interactions result in the more rapid and complete conversion of SN-38 to the carboxylate form [11]. This information demonstrates the importance of simultaneous quantitation of the carboxylate and lactone forms of SN-38. To date, several methods have been described for such determinations [12–18]. Direct measurement of the carboxylate form was impossible with these methods except that in Ref. [15], because it was eluted with the solvent front during HPLC separation. Therefore, carboxylate concentrations were estimated based on total lactone concentrations following acidification of the sample. In the present paper, we report a new and simple HPLC method using a C_{18} column and ordinary buffer systems without an ion-pairing agent.

About 10 cell lines have hitherto been reported to be resistant to CPT-11 or SN-38 [19,20]. Several in vitro mechanisms of resistance to CPT-11 or SN-38 have been reported. The resistant cell lines play an important role in elucidating the in vivo drug resistance mechanism, although results from experiments using resistant cell lines do not always accurately reflect the phenomenon.

Table 1
Characteristics of 15 derivatives

Compound	Structure		Ratio of fluorescence intensity	
	X	Y	Em_{max} (nm)	Carboxylate/lactone
SN-38	OH	H	543	1.2/1.0 (1.2)
SN-22	H	H	439	3.4/2.1 (1.6)
SN-343	Me	H	434	20.7/10.9 (1.9)
SN-348	Br	H	438	3.4/2.4 (1.4)
SN-349	Cl	H	436	17.4/14.1 (1.2)
SN-392	NH_2	H	527	1.0/1.6 (0.6)
SN-351	H	Br	438	2.7/2.1 (1.3)
SN-352	H	Cl	434	16.6/15.0 (1.1)
SN-353	H	F	432	19.3/14.0 (1.4)
SN-355	H	OH	440	0.5/0.5 (1.0)
SN-364	Cl	Cl	442	2.9/4.5 (0.6)
SN-398	OH	F	534	2.8/1.4 (2.0)
SN-397	OMe	F	416	35.1/32.6 (1.1)
SN-443	Me	F	434	23.5/14.7 (1.6)
SN-444	F	F	436	17.0/11.1 (1.5)

Excitation, 380 nm.

Fourteen derivatives of camptothecin were recently developed by Yakult Honsha (Table 1). These derivatives were synthesized by replacing the hydroxy residue with others (hydrogen, halogen methyl, methoxy residues, etc.) to overcome SN-38 resistance. In the present study, we have developed a new HPLC method to measure cellular concentrations of other derivatives to gain insight into the correlation between cellular concentrations with retention on the C_{18} column. Information of the relationship between the chemical properties and antitumor activities of these 14 compounds would provide a useful path to the development of new antitumor drugs.

2. Experimental

2.1. Materials and reagents

SN-38 and 14 new derivatives of camptothecin (Table 1) were provided by Yakult Honsha. The method of synthesis will be reported elsewhere. Dimethyl sulfoxide (DMSO) was purchased from Nacalai Tesque (Kyoto, Japan). The water used was

of Milli-Q grade, and all other chemicals were of analytical or HPLC grade.

2.2. Cell lines and growth conditions

The human non-small-cell lung cancer cell line PC-6 was kindly donated by Dr. M. Oka (Nagasaki University). PC-6 is selected for the reason that it is the parent of PC-6/SN2-5H, which has high breast cancer resistant protein (BCRP), although PC-6 has less BCRP. The purpose of our project is an elucidation of the mechanism of ATP-dependent SN-38 transport activities of BCRP and a development of new resistant drugs against BCRP. This HPLC method was developed for the project. The doubling time of PC-6 cells was 23 h. The cell line was maintained as monolayers in RPMI 1640 medium (Gibco BRL, Grand Island, NY, USA) supplemented with 10% fetal calf serum (FCS, Gibco BRL) as described previously [21].

2.3. Fluorescence intensity

Fluorescence spectra were measured using a Hitachi F-4010 Fluorescence spectrometer (Hitachi, Tokyo, Japan).

2.4. Apparatus

The HPLC system consisted of a Jasco PU1580 pump, a Jasco FP920 fluorescence detector (Jasco, Tokyo, Japan) and a Shimadzu C-R4A integrator (Shimadzu, Kyoto, Japan). Isocratic elutions were performed using a Mightysil RP-18 (L) GP column (5 μm, 150 mm×4.6 mm I.D.; Kanto Chemical, Tokyo, Japan) with a guard column (5 μm, 5 mm× 4.6 mm I.D.). The excitation and emission wavelengths were 380 and 550 nm, respectively, for SN-38, SN-392, and SN-398. Emission wavelength was set at 440 nm for the other 12 compounds. The mobile phase for separation of SN-38 consisted of 50 m*M* phosphate buffer (pH 6.0)–acetonitrile–tetrahydrofuran (THF) (80:20:2, v/v). For the derivative compounds, the ratio of acetonitrile was adjusted to achieve an analyte retention time of 12–18 min. The flow-rate was 1.0 ml/min and all separations were carried out at room temperature (23–25 °C).

2.5. Sample preparation of standard solutions

The method of quantitation used external standards. Stock solutions containing 2.5 m*M* of the derivative in DMSO were prepared and stored at −20 °C. A 20-μl aliquot of stock solution was diluted with 980 μl of 0.01 *M* phosphate buffer (pH 3.0) for the lactone form or 0.05 *M* sodium hydroxide (NaOH) for the carboxylate form. HPLC analysis determined that these secondary stock solutions, 50 μ*M*, were 95% stable for at least 2 months at −20 °C. Sequential dilutions of 5.0, 0.5, 0.05 μ*M* were always freshly prepared by diluting each 50 μ*M* solution with the appropriate buffer. These diluted solutions were allowed to stand at room temperature for at least 30 min to ensure equilibration. All stock and standard solutions were stored in polypropylene tubes, in order to prevent concentration decreases by adsorption of the drugs, particularly the lactone form, to the containers.

2.6. SN-38 sample preparation for determination of cellular concentrations

Cells (1×10^6) were incubated at 37 °C for 1, 5, 10 or 20 min in the presence of 10 μ*M* carboxylate form of SN-38 in 200 μl of RPMI 1640 medium supplemented with 50 m*M* Hepes/Tris (pH 7.4) and then washed twice in 800 μl of ice-cold PBS(−). After centrifugation at 15 000 *g* for 5 min at 4 °C, cells were disrupted by vigorous sonication in 200 μl of distilled water (pH 6.0), freezing with liquid N_2 and rapid thawing. This was carried out three times and the cell solution was centrifuged at 15 000 *g* for 5 min at 4 °C. The supernatant was then subjected to HPLC. The reason we use distilled water as the disruptive solution of cells is that the distilled water has a pH of 6.0 and low enough molarity to disrupt cells. Moreover, both lactone and carboxylate forms are stable (above 98%) in distilled water for 2 h at room temperature (data not shown).

2.7. Method validation

The within- and between-day reproducibilities were determined for the carboxylate and lactone forms of SN-38. Three different concentrations of both forms of SN-38 were analyzed. Three aliquots

of each sample were analyzed each day for 6 days, and the resulting coefficients of variation (C.V.) and accuracy indicated the within- and between-day reproducibilities.

The limit of detection was defined as the concentration of carboxylate form resulting in a signal-to-noise ratio of 5.

3. Results and discussion

3.1. Detectable emission of derivatives of SN-38

Wavelength optimization revealed that the maximum emission wavelength of the derivatives were different from that of SN-38, when the appropriate excitation wavelength, i.e. 380 nm, was used (Fig. 2). SN-38 derivatives were classified into two groups. One was the SN-38 type that has two emission peaks at around 543 nm (SN-392, SN-398). SN-398 had a similar pattern as SN-38 and the carboxylate form showed a twofold higher fluorescence intensity than the lactone form. On the other hand, the SN-392 carboxylate form had a lower fluorescence intensity than the lactone form. The second group was the SN-22 type that showed a maximum intensity at around 439 nm (SN-355, SN-364, etc.). Although the SN-22 carboxylate form had a higher fluorescence intensity than the lactone form, the lactone form of SN-364 showed a higher intensity than its carboxylate form. Table 2 shows that each derivative has a different maximum emission wavelength, and a different ratio of fluorescence intensity for the carboxylate and lactone forms. The excitation and emission wavelengths were set at 380 and 550 nm for SN-38, SN-392, SN-398, and the emission wavelength was set at 440 nm for the other 12 compounds.

3.2. Method optimization

3.2.1. Effect of acetonitrile and THF

SN-355, a derivative with a hydroxy group in the Y position, was difficult to elute from the ODS column due to strong adsorption. However, addition of THF at 2 ml per 100 ml of acetonitrile–phosphate buffer (pH 6.0) with an increase in the acetonitrile ratio led to more rapid elution of the lactone form

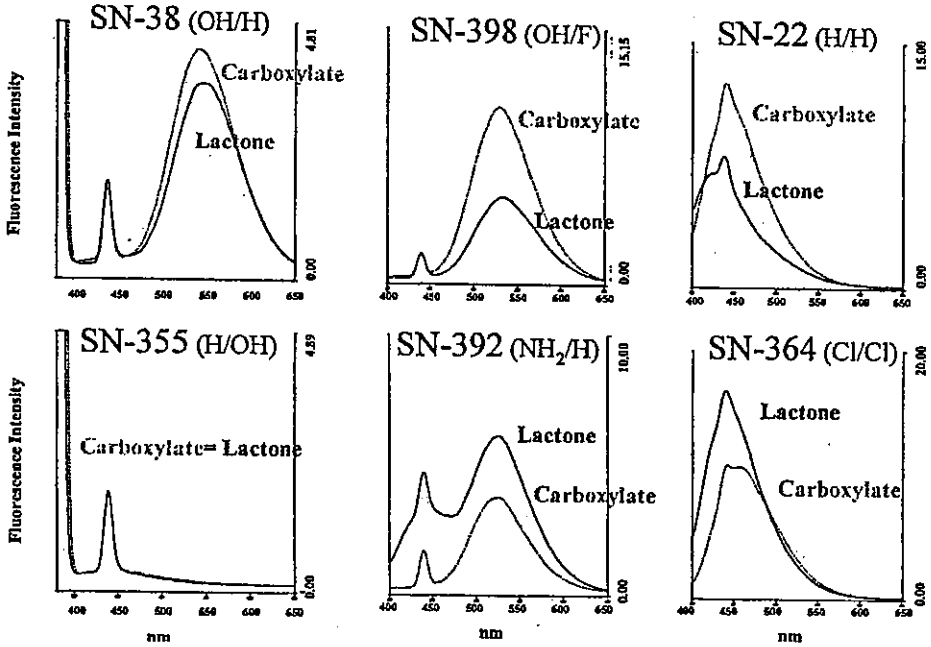

Fig. 2. Representative fluorescent spectrum of SN-38 and five derivatives. Fluorescence spectra were measured using a Hitachi F-4010. The appropriate excitation wavelength, i.e. 380 nm was used.

Table 2
HPLC conditions for SN-38 derivatives

0.05 *M* Phosphate buffer–acetonitrile–THF	Em (Ex: 380 nm)	SN-38 derivatives
80:20:2	550 nm	SN-38, SN-392, SN-398
70:30:2	440 nm	SN-22, SN-353, SN-355
60:40:2	440 nm	SN-443, SN-444, SN-349
		SN-348, SN-343, SN-352
		SN-351, SN-364, SN-397

(Fig. 3). Furthermore, the lactone forms of low-polarity derivatives with halogens were eluted in around 20 min by increasing the acetonitrile ratio up to 30 or 40% (Table 2).

3.2.2. Column selection

For column selection, we evaluated four ODS HPLC columns (4.6 mm I.D.×150 mm) under identical conditions (Fig. 4). The mobile phase consisted of 50 m*M* phosphate buffer (pH 6.0)–acetonitrile–THF (80:20:2, v/v). Samples were 10 μl of 100 pmol/ml of the carboxylate and lactone forms of SN-38. In this experiment samples were prepared separately and injected in turn into the same injector loop. As soon as the end of the injection, separations were started. The conversion between carboxylate and lactone does not occur in the mobile phase (pH 6.0) for at least 30 min (data not shown). On column A (TSK-gel ODS 80Ts), carboxylate and lactone forms eluted at 3.44 min and 23.27 min, respectively (resolution value (R_s)=5.73). This was unsuitable for this investigation because the lactone peak was late and broad. Column B (J's sphere ODS-H80, S-4 μm, 8 nm) gave good resolution (R_s=20.8) but was unsuitable due to solvent shock occurring just prior to carboxylate form elution. The retention time on column C (Waters Puresil C_{18}, 5 μ, 120 Å) was not long enough. Carboxylate and lactone forms were eluted at 2.54 min and 7.63 min, respectively (R_s=5.45) and the carboxylate form could not be separated from cellular components. On the Mightysil RP-18 (L) GP column (column D) good separation was observed (R_s=10.39). We finally decided to select the Mightysil RP-18 (L) GP column because of its high separation capacity and reasonable cost (50% less than the others).

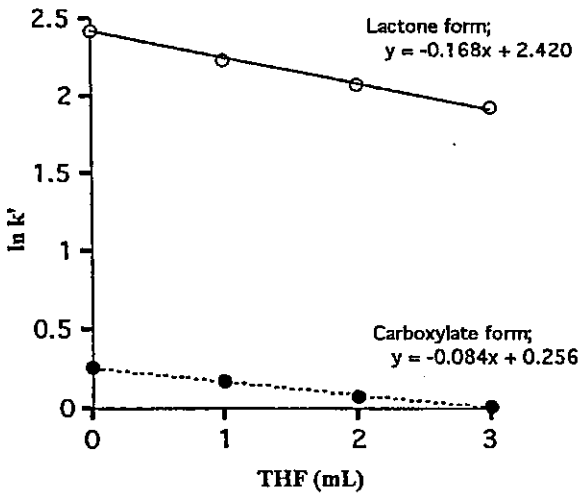

Fig. 3. Effect of tetrahydrofuran (THF) on capacity factor (k') of SN-355. The *X*-axis presents additional volume (ml) per 100 ml of acetonitrile–phosphate buffer (pH 6.0). $k' = (t_R - t_0)/t_0$, where t_R is the retention time of the compound and t_0 is the retention time of unretained molecules. HPLC conditions, the excitation and emission wavelengths were 380 and 440 nm, respectively. The mobile phase consisted of 50 m*M* phosphate buffer (pH 6.0)–acetonitrile–THF (70:30:0–3, v/v). The flow-rate was 1.0 ml/min and all separations were carried out at room temperature (23–25 °C).

3.2.3. Optimum pH

To estimate the stability of SN-38 in elution buffer, we investigated the conversion ratio of SN-38 from the lactone to the carboxylate form in 10 m*M* phosphate buffer after 30 min at pH 3.0 to 9.0 (Fig. 5). The lactone form was stable at pH below 6.0, whereas it started to decrease and rapidly convert to carboxylate in the pH range of 7.0 to 9.0. However, the carboxylate form slowly converted to lactone from pH 9.0 and completely disappeared at pH 3.0. These results indicated that the conversion rate depends on the hydrogen ion concentration. The conversion rate of lactone to carboxylate was substantially delayed in 0.1 *M* phosphate buffer with 97% of the original form existing at pH 7.4 after 30

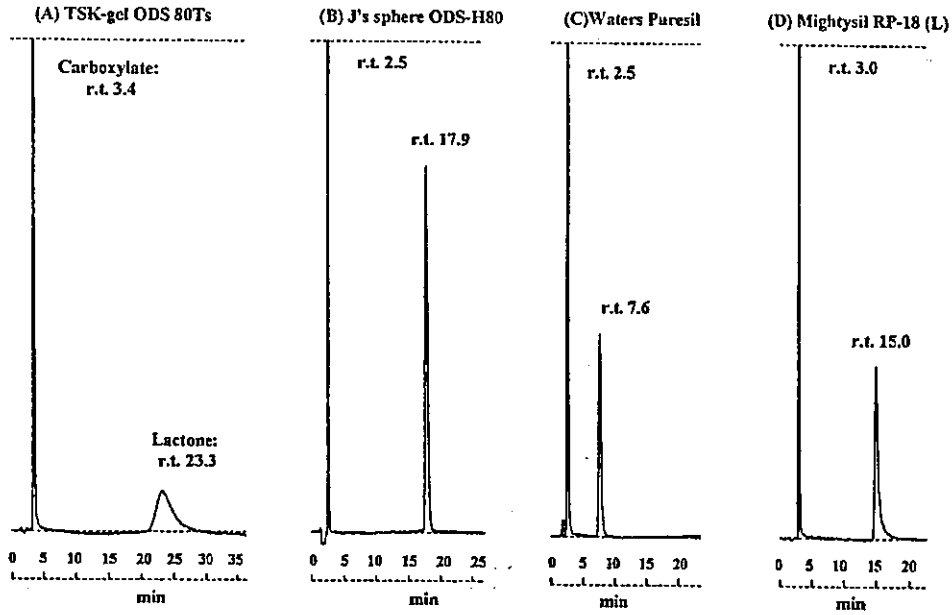

Fig. 4. Comparison of columns for separation of SN-38 carboxylate and lactone forms. Column A, TSK-gel ODS 80Ts (5 μm); B, J's sphere ODS-H80 (S-4 μm, 8 nm); C, Waters Puresil C_{18} (5 μ, 120 Å); D, Mightysil RP-18 (L) GP column (5 μm). HPLC conditions, the excitation and emission wavelengths were 380 and 550 nm, respectively. The mobile phase consisted of 50 m*M* phosphate buffer (pH 6.0)–acetonitrile–THF (80:20:2, v/v). The flow-rate was 1.0 ml/min and all separations were carried out at room temperature (23–25 °C).

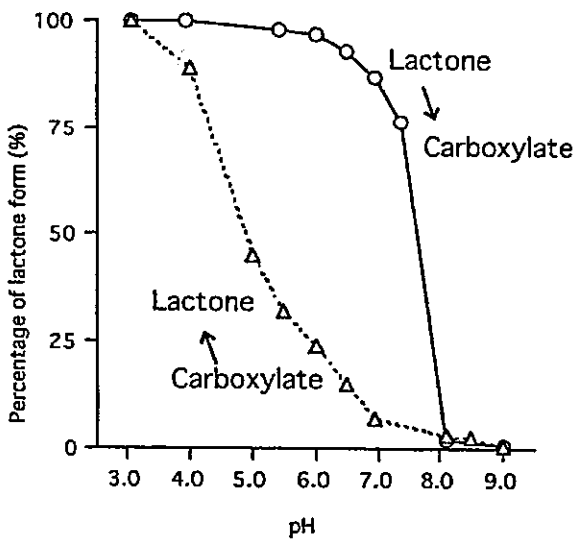

Fig. 5. Conversion ratio between lactone and carboxylate form. Conversion ratio is shown as percentage (%) of lactone form in total SN-38 concentration at each pH in 10 m*M* phosphate buffer after 30 min mixture at room temperature.

min. From these results, the pH of the elution buffer was adjusted to 6.0 and the buffer concentration was set to 50 m*M* to maintain the stability of the SN-38 lactone form. The stability of the lactone form in eluent containing acetonitrile and THF at 15 min, 60 min and 24 h was 99.3%, 97.9% and 90.0%, respectively.

3.2.4. Chromatography

Fig. 6 shows typical chromatograms of carboxylate and lactone forms of SN-38. The retention time of carboxylate and lactone were 3.0 and 15.0 min, respectively. Fig. 6A is 100 μl of supernatant of blank cell lysates. Fig. 6B or C are blank cell lysates with 10 pmol/ml carboxylate or lactone form of SN-38 in the same volume as Fig. 6A. Fig. 6D is a sample of a supernatant of cellular lysates at 1 min into the experiment (see detail in Section 2.6). A mass injection volume (100 μl) gave a dull peak of lactone form.

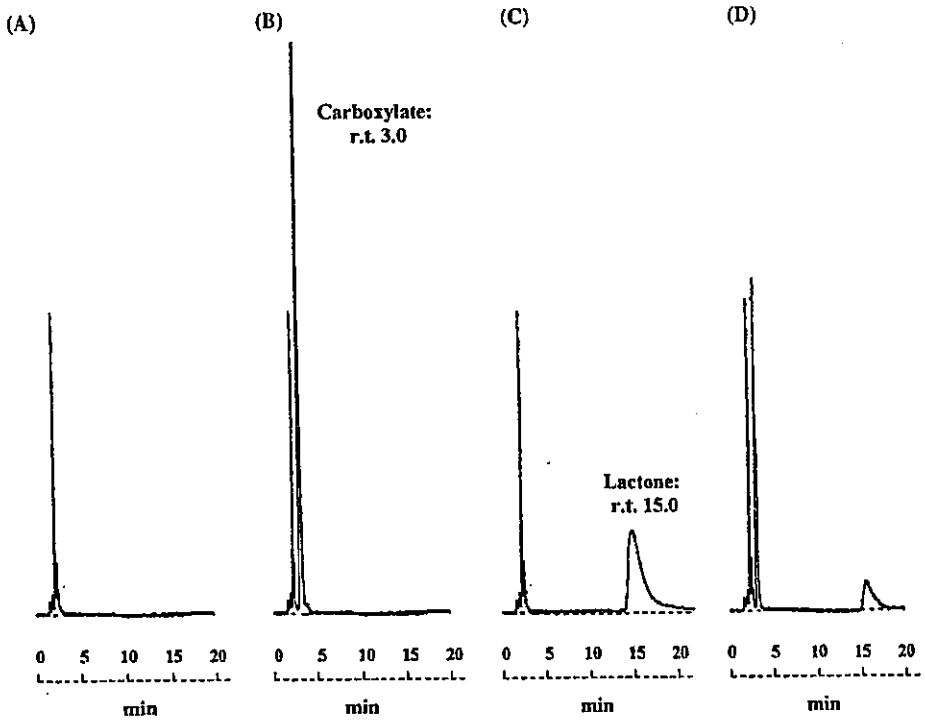

Fig. 6. HPLC chromatograms of carboxylate and lactone form of SN-38. (A) Chromatogram of supernatant of blank cell lysates; (B, C) blank cell lysates with 10 pmol/ml carboxylate or lactone form of SN-38 in the same volume as (A) for a calibration curve; (D) sample of a supernatant of cellular lysates at 1 min of experiment (see detail in Section 2.6).

3.3. Method validation

Within- and between-day reproducibilities for the carboxylate and lactone forms of SN-38 solutions are shown in Table 3. The coefficient of variation (C.V.) of peak areas for each was less than 3%. The accuracy of the method (within-day), expressed by the bias, varied between −1.0 and 1.1% for carboxylate form, and between −0.2 and 1.7% for lactone form, respectively. The between-day accuracy varied between −5.5 and −1.8% for carboxylate form, and between 3.7 and 4.1% for lactone form, respectively. This result suggests that the carboxylate form degraded within a few days.

The linearity study was carried out with concentrations ranging from 4 to 5000 pmol/ml of either the carboxylate form in 0.05 *M* NaOH or the lactone form in DMSO. The linearity of the calibration lines obtained by plotting peak areas against concentration was examined. The equations for the carboxylate and lactone forms of SN-38 were $y = 2362.5x + 330.6$

Table 3
Precision (C.V.) and accuracy (bias) in the HPLC assay

Concentration (pmol/ml)	Carboxylate ($n=3$)		Lactone ($n=3$)	
	C.V. (%)	Bias	C.V. (%)	Bias
Within-day				
50	2.1	−1.0	2.7	1.7
500	2.3	1.1	1.7	−0.2
5000	1.0	0.0	1.5	0.0
Between-day				
50	0.9	−5.5	2.5	4.0
500	2.6	−1.8	2.7	4.1
5000	2.5	−2.8	3.0	3.7

($r^2 = 1.000$) and $y = 3074.5x - 2292$ ($r^2 = 1.000$), respectively. The limit of quantitation (LOQ) was ~4.0 pmol/ml (1.6 ng/ml) for both forms.

3.4. Stability of SN-38 solution

To quantitate the cellular concentrations of the SN-38 lactone form, an aliquot of lactone form solution in 10 m*M* acetate buffer (pH 3.0) was added to several solvents. The stability of the SN-38 lactone form at 37 °C in water (pH 6.0), PBS (pH 7.4), human plasma (pH 7.4) and RPMI 1640 (pH 7.4) using this HPLC method is shown in Fig. 7. In water the proportion of lactone form remained unchanged for 3 h, and thus water is the most suitable solution for sample preparation prior to HPLC quantitation. The half-life ($t_{1/2}$) values of the SN-38 lactone form in PBS, human plasma and RPMI 1640 medium were 0.51, 0.63 and 0.26 h, respectively.

3.4.1. Quantitation of cellular SN-38 concentration

To estimate the ratio of carboxylate/lactone forms of SN-38 in PC-6 cells, we measured the cellular concentrations of the carboxylate and lactone forms after incubation with 10 m*M* of SN-38 (Fig. 8). The lactone form accounted for about 50% of the total cellular SN-38 concentration. However, in the RPMI medium, the concentration ratio of the SN-38 carboxylate form to the lactone form was 97:3. These results suggested that a large portion of the carboxylate form was converted to the lactone form

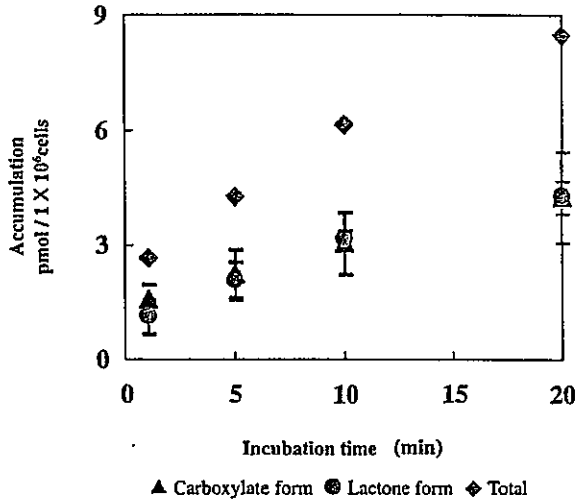

Fig. 8. Cellular concentration of SN-38 in PC-6 cells. Accumulation is shown as cellular concentrations of each form of SN-38 in PC-6 cells (1×10^6) after incubation for 1, 5, 10, 20 min at 37 °C.

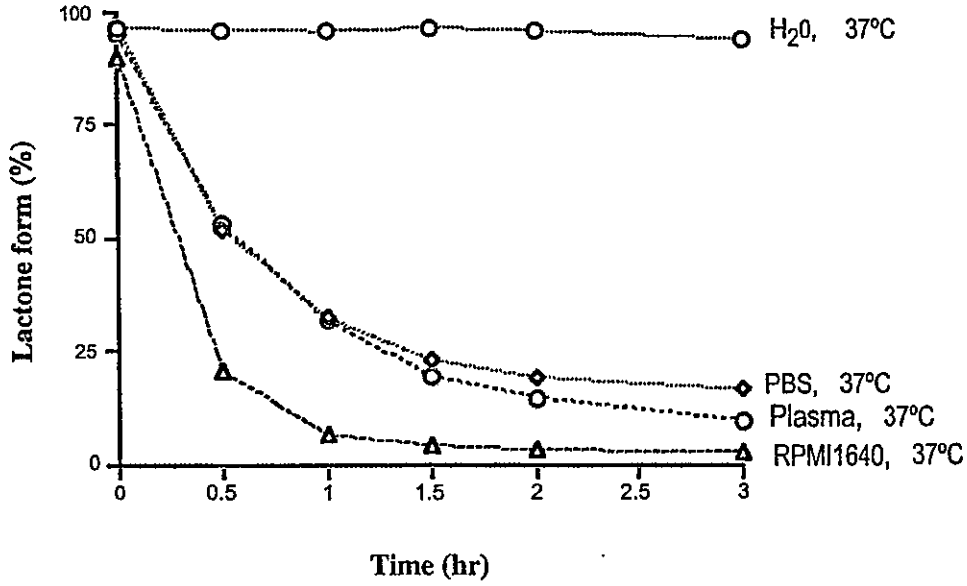

Fig. 7. Stability of SN-38 lactone form in several solutions. Alteration of the SN-38 lactone form concentrations after addition to water (pH 6.0), PBS (pH 7.4), human plasma (pH 7.4) and RPMI 1640 (pH 7.4) for 0.5, 1, 1.5, 2 and 3 h at 37 °C.

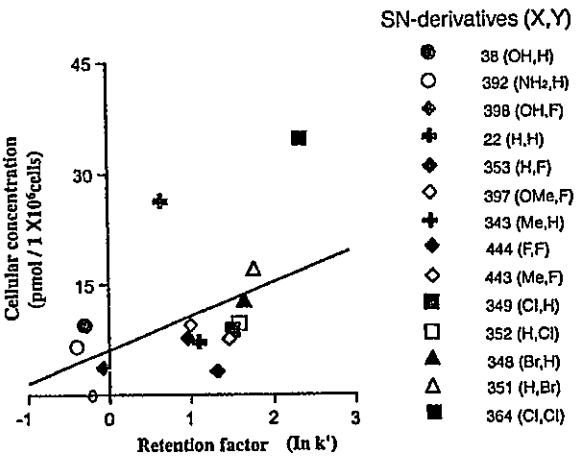

Fig. 9. Relationship between HPLC retention factors (ln k') and the cellular concentration of SN-38 and the other 14 derivatives in PC-6 cells.

under acidic cellular conditions, or that only the lactone form was taken up into cells. A follow-up study is currently underway to investigate this further.

3.5. Interrelation between cellular concentrations of derivatives and HPLC retention

The 15 SN-38 derivatives were separated under the same conditions; 50 mM phosphate buffer (pH 6.0)–acetonitrile–tetrahydrofuran (THF) in a ratio of 60:40:2 (v/v). The HPLC retention factors (ln k') were plotted against cellular concentrations in the PC-6 cell line (Fig. 9). A weak linear relationship between the HPLC retention factors (ln k') and the cellular concentrations of these compounds was observed ($Y = 4.875X + 6.568$, $r^2 = 0.202$). This result suggests that low-polarity compounds tend to accumulate in cells.

4. Concluding remarks

We have described a simple and cost-effective HPLC method without an ion-pairing agent that allows the simultaneous determination of the lactone and carboxylate forms of SN-38 and 14 SN-38 derivatives. Using this HPLC method, we determined the cellular concentrations of the lactone and carboxylate forms of SN-38. A linear relationship between ln k' and cellular concentrations of these compounds was observed. This suggests that low-polarity compounds easily accumulate in cells and can overcome drug resistance. Our new HPLC method will be useful for investigations related to the breast cancer resistance protein (BCRP) ABCG2, a transporter that exports SN-38 [21,22]. Furthermore, this observation provides valuable insight into derivative synthesis and chemical modification of antitumor drugs.

References

[1] S. Sawada, S. Okajima, R. Aiyama, K.-I. Nokata, T. Furuta, T. Yokokura, E. Sugino, K. Yamaguchi, T. Miyasaka, Chem. Pharm. Bull. 39 (1991) 1446.
[2] M. Wall, M. Wani, C. Cook, K. Palmer, A. McPhail, G. Slim, J. Am. Chem. Soc. 88 (1966) 3888.
[3] Y.-H. Hsiang, R. Hertzberg, S. Hecht, L.F. Liu, J. Biol. Chem. 260 (1985) 14873.
[4] R.P. Hertzberg, R.W. Busby, M.-J. Caranfa, K.G. Holden, R.K. Johnson, S.M. Hecht, W.D. Kingsbury, J. Biol. Chem. 265 (1990) 287.
[5] M. Redinbo, L. Stewart, P. Kuhn, J. Champoux, W. Holl, Science 279 (1998) 1504.
[6] L. Stewart, M. Redinbo, X. Qui, W. Hol, J. Champoux, Science 279 (1998) 1534.
[7] Y. Kawato, M. Aonuma, Y. Hirota, H. Kuga, K. Sato, Cancer Res. 51 (1991) 4187.
[8] W.J. Slichennmyer, E.K. Rowinsky, R.C. Donehower, S.H. Kaufmann, J. Natl. Cancer Inst. 85 (1993) 271.
[9] J. Fassberg, V.J. Stella, J. Pharm. Sci. 81 (1992) 676.
[10] T.G. Burke, Z. Mi, Anal. Biochem. 212 (1993) 285.
[11] Z. Mi, T.G. Burke, Biochemistry 33 (1994) 10325.
[12] L.P. Rivory, J. Robert, J. Chromatogr. B 661 (1994) 133.
[13] Y. Sasaki, Y. Yoshida, K. Sudoh, H. Hakusui, H. Fujii, T. Ohtsu, H. Wakita, T. Igarashi, K. Itoh, Jpn. J. Cancer Res. 86 (1995) 111.
[14] X.-Y. Chu, Y. Kato, K. Niinuma, K. Sudo, H. Hakusui, Y. Sugiyama, J. Pharmacol. Exp. Ther. 281 (1997) 304.
[15] N. Kaneda, Y. Hosokawa, T. Yokokura, Biol. Pharm. Bull. 20 (1997) 815.
[16] D.L. Warner, T.G. Burke, J. Chromatogr. B 691 (1997) 161.
[17] A. Kurita, N. Kaneda, J. Chromatogr. B 724 (1999) 335.
[18] G. Boyd, J.F. Smyth, D.I. Jodrell, J. Cummings, Anal. Biochem. 297 (2001) 15.
[19] T. Andoh, K. Ishii, Y. Suzuki, Y. Ikegami, Y. Kurunoki, Y. Takemoto, K. Okada, Proc. Natl. Acad. Sci. USA 84 (1987) 5565.
[20] A. Fujimori, M. Gupta, Y. Hori, Y. Pommir, Mol. Pharmacol. 50 (1996) 1472.

[21] K. Nakatomi, M. Yoshikawa, M. Oka, Y. Ikegami, S. Hayasaka, K. Sano, K. Shiozawa, S. Kawabata, H. Soda, T. Ishikawa, S. Tanabe, S. Kohno, Biochem. Biophys. Res. Commun. 288 (2001) 827.

[22] S. Kawabata, M. Oka, K. Shiozawa, K. Tsukamoto, K. Nakatomi, H. Soda, M. Fukuda, Y. Ikegami, K. Sugahara, Y. Yamada, S. Kamihira, L.A. Doyle, D.D. Ross, S. Kohno, Biochem. Biophys. Res. Commun. 280 (2001) 1216.

Chem-Bio Informatics Journal, Vol. 3, No. 4, pp.175-193(2003)

High-Speed Screening and Structure-Activity Relationship Analysis for the Substrate Specificity of P-Glycoprotein (ABCB1)*

Yuko Onishi[1,2], Hiroyuki Hirano[2], Kunio Nakata[1], Keisuke Oosumi[3], Makoto Nagakura[3], Shigeki Tarui[2], and Toshihisa Ishikawa[1*]

1) Department of Biomolecular Engineering, Graduate School of Bioscience and Biotechnology, Tokyo Institute of Technology, Nagatsuta, Yokohama 226-8501, Japan
2) GS PlatZ Co. Ltd., 1-7-11 Nihonbashi, Chuo-ku, Tokyo 103-0027, Japan
3) BioTec Co. Ltd, 2-29-4 Yushima, Bunkyo-ku, Tokyo 113-0034, Japan

**E-mail: tishikaw@bio.titech.ac.jp*

(Received November 4, 2003; accepted December 18, 2003; published online December 31, 2003)

Abstract

Human ABCB1 (P-glycoprotein or MDR1) mediates the elimination of a variety of drugs from cells and thereby plays a critical role in determining the pharmacokinetic profiles of drugs in our body. In the present study, we have developed a high-speed screening system to investigate the substrate specificity of ABCB1 towards a variety of drugs and compounds. The plasma membrane fraction of Sf9 insect cells overexpressing human ABCB1 was used to measure the ATPase activity. Among 41 different compounds and therapeutic drugs tested in this study, Ca^{2+} channel blockers, such as verapamil, bepridil, fendiline, prenylamine, and nicardipine, stimulated the ATPase activity. Doxorubicin, paclitaxel, quinidine, and FK506 also stimulated the ABCB1 ATPase activity, although to an extent relatively smaller than that of the Ca^{2+} channel blockers. We have measured the surface activity of those 41 different compounds. A two-dimensional plot of the air-water partition coefficient (K_{aw}) vs. ABCB1 ATPase activity clearly classified those compounds into two groups; namely, ABCB1 substrate and non-substrate groups. ABCB1 substrates were found to have a log K_{aw} value higher than 4.3. Based on the ABCB1 ATPase activity, we have analyzed structure-activity relationships (SAR) for a total of 37 different compounds. The multiple linear regression analysis delineates a clear relationship between the ABCB1 ATPase activity and the chemical fragmentation codes. Thereby, we have identified multiple sets of chemical fragmentation codes closely related with the substrate specificity of ABCB1. This approach is considered to be practical and useful for the molecular design of such new drugs that can penetrate the blood-brain-barrier or circumvent the multidrug resistance of human cancer.

Key Words: P-glycoprotein, high-throughput screening (HTS), structure-activity relationship (SAR), chemical fragmentation code
Area of Interest: Information and Computing Infrastructure for Drug Design and Toxicology

1. Introduction

Accumulating evidence suggests that drug transporters play pivotal roles in determining the pharmacokinetic profiles of drugs and, by extension, their overall pharmacological effects (i.e., drug absorption, drug distribution, and elimination, drug concentration at the target site, and the number and morphology of target receptors) [1][2][3][4]. The effects of drug transporters on the pharmacokinetic profile of a drug depend on their expression and functionality.

Human ABCB1 (P-glycoprotein or MDR1), one of the drug transporters, was originally identified because of its overexpression in cultured cancer cells associated with an acquired cross-resistance to multiple anticancer drugs [5][6]. While "P-glycoprotein" was initially thought to play a role in modulating cellular permeability ('P' stands for permeability) to drugs, it has later been demonstrated to be an ATP-dependent efflux pump of hydrophobic anticancer drugs including colchicine, doxorubicin, daunorubicin, vincristine, and etoposide (VP-16). Historically P-glycoprotein provided one of the mechanistic explanations for the multidrug resistance phenomeon. The function of ABCB1 as a mechanism of multidrug resistance has been extensively investigated [7]. It was assumed that ABCB1 functions as a membrane pore to export intracellularly located substrate. Subsequently, another model has been proposed where ABCB1 translocates a substrate from the inner leaflet side of the membrane to the outer leaflet side; thus, it functions as a flippase or membrane vacuum cleaner.

Cells selected *in vitro* against a lipophilic cytotoxic compound usually develop cross-resistance to other drugs. Some multidrug-resistant cell lines are significantly more resistant to the drug used in their selection than to the other drugs. It is important to know that ABCB1 is expressed not only in cancer cells but also in many normal tissues. For example, it is located in the apical domain of the enterocytes of the gastrointestinal tract (jejunum and duodenum) and limits the uptake and absorption of drugs and other substrates from the intestine into the systemic circulation by excreting substrates into the gastrointestinal tract. Likewise, the expression of ABCB1 on the lumenal membrane of capillary endothelial cells of the brain restricts drug distribution into the central nervous system. This function appears to be very important in protecting the central nervous system from the attack of toxic compounds. Evidence for the protective role of ABCB1 in the blood-brain barrier has been demonstrated in several studies with *mdr1a* knockout mice [8]. A similar protective role to limit the distribution of potentially toxic xenobiotics into tissues was suggested for ABCB1 expression in the placenta and the testis. ABCB1 expressed in the canalicular domain of hepatocytes and the brush border of proximal renal tubules plays a role in the biliary and urinary excretion of xenobiotics and endogenous compounds.

ABCB1 is intrinsically involved in the function of the blood-brain barrier, which prevents lipophilic xenobiotics and many therapeutics drugs from entering the central nervous system. Furthermore, low bioavailability or slow intestinal absorption of drugs is often due to the efflux of drugs mediated by ABCB1. Such phenomena are critical for the development of therapeutics drugs. Hence, there is a considerable demand for rapid and efficient *in vitro* assay systems and computational methods to assess biopharmaceutical properties of test compounds.

In the present study, we have developed a high speed screening method for analyzing the substrate specificity of ABCB1. Our approach is to measure the stimulation of ATPase activity by ABCB1 substrates in plasma membranes prepared from ABCB1–overexpressing Sf9 insect cells. Furthermore, we have developed a computational program that analyses the structure–activity relationship (SAR) for the ATPase activity of structurally diverse substrates of ABCB1.